Image Features Extraction of Gas/liquid Two-Phase Flow in Horizontal Pipeline by GLCM and GLGCM

Hongyi Wang Feng Dong
（Tianjin Key Laboratory of Process Measurement and Control, School of Electrical Engineering and Automation
Tianjin University, Tianjin 300072, China）
Email: *fdong@tju.edu.cn*

Abstract *–Gray level co-occurrence matrix (GLCM) and the gray level-gradient co-occurrence matrix (GLGCM) were used to analyze gas/liquid flow images. Gas/liquid two-phase flow experiments were practiced and high-speed images were captured. A set of textural features were extracted from the GLCM and GLGCM. Examples of experimental results confirm the effectiveness of several features among them. All of the effective textural features have a relation with the gas/liquid density ratio, but not relate to the superficial velocity of gas or liquid.*

Key words *– gas/liquid two-phase flow, gas/liquid density ratio, textural feature, GLCM, GLGCM.*

I. INTRODUCTION

Gas/liquid two-phase flow research has received great attention in the research field of multi-phase flow for its conmen appearance in many industry processes and fundamental role to multi-phase flow [1]. The widespread presence of these multi-fluid systems suggests the utility of a general technique of description to understand their behavior.

There are already some detecting methods for two phase flow measurement. Such as, microwave, radiation, process tomograph, correlation technology, and so on [2] [3]. However, all these methods have their application limits. In the present study we focus on gas-liquid two-phase flow characters study by image texture analysis method.

Texture is an important property for the classification of images and can be regarded as the pattern of gray level tones present in an image. Image analysis has been used extensively to detect textural features in biomedical applications [4-8] and terrain classification applications [9-12]. Textural feature features have been evaluated by several methods with statistical method, structure method and frequency spectrum method in general. In two-phase flow filed, Zhou Yunlong [13] and Wang Zhenya [14] have already successfully used the gray level co-occurrence matrix in image features extraction for flow regime recognition.

In this paper, gray level co-occurrence matrix (GLCM) and the gray level-gradient co-occurrence matrix (GLGCM) were applied to analyze the flow texture of the gas/liquid two-phase flow. Experiments were carried out with high-speed camera recording system. Gas/liquid two-phase flow images were processed by digital image processing method. Texture features of the experimental images were extracted and analyzed by GLCM and GLGCM respectively. The features which could reflect gas-liquid flow characters clearly were shown in the paper. And relative discussion was carried on the results.

978-1-4244-3864-8/09/$25.00 ©2009 IEEE

II. METHODS FOR FEATURES EXTRACTION

GLCM and GLGCM are detailed in this section. Both of the two methods capture the second order statistics of local image features. The difference is that GLCM captures the second order statistics of gray level values while GLGCM captures that of gray level gradients. The formula of textural features based on GLCM and GLGCM were described in the following section for experimental image analysis.

A. Gray level co-occurrence matrix

Gray level co-occurrence matrix (GLCM) has been employed in extracting texture features and various image processing applications for a long time. Co-occurrence matrixes which describe the gray level spatial dependency in two dimensional images have been presented in [15].

GLCM could reflect image's synthetically gray information about direction, interval, changing extent and so on.

As to a M*N digital image, GLCM are constructed to record the joint probability $p(i, j)$ with which two neighboring pixels in the image, one with gray level i and the other with gray level j in direction θ and distance d. Usually, we set $\theta = 0^o, 45^o, 90^o, 135^o, d = 1$. The definition of the co-occurrence matrix is shown in the following:

$$P(i, j, d, \theta) = \{[(x, y), (x + \Delta x, y + \Delta y)] \mid f(x, y) = i, f(x + \Delta x, y + \Delta y) = j; x = 1,2,\cdots M; y = 1,2,\cdots N\} \quad (1)$$

Where, $i, j = 0,1,\cdots L-1$; x, y is the coordinate of pixel; L is the gray level and $L = 256$ in this research. As above vectors have difference meanings and range, it is necessary to do the inner normalization before storing into the database. For simple, direction θ and

distance d is elided in GLCM expression in the following discussion.

As a character token for image texture analysis, GLCM is not applied directly, but calculates the second-order statistics based on the GLCM. Haralick proposed 14 statistical features extracted from the GLCM, here we select 7 from that and shown in table 1.

Table 1. Textural features by GLCM

Serial No.	Texture Features	Calculating formula
1	contrast	$f_1 = -\sum_{i=0}^{L-1}\sum_{j=0}^{L-1}\|i-j\|^2 P_{ij}$
2	entropy	$f_2 = -\sum_{i=0}^{L-1}\sum_{j=0}^{L-1} P_{ij}\, log_2\, P_{ij}$
3	energy	$f_5 = \sum_{i=0}^{L-1}\sum_{j=0}^{L-1} P_{ij}^2$
4	homogeneity	$f_3 = -\sum_{i=0}^{L-1}\sum_{j=0}^{L-1}\frac{P_{ij}}{1+\|i-j\|^2}$, k>=1
5	correlation	$f_4 = \frac{1}{\sigma_x\sigma_y}\sum_{i=0}^{L-1}\sum_{j=0}^{L-1}(i\cdot j)P_{ij} - \mu_x\mu_y$, $\mu_x = \sum_{i=0}^{L-1} i\sum_{j=0}^{L-1} P_{ij}$, $\mu_y = \sum_{j=0}^{L-1} j\sum_{i=0}^{L-1} P_{ij}$, $\sigma_x^2 = \sum_{i=0}^{L-1}(i-\mu_x)^2\sum_{j=0}^{L-1} P_{ij}$, $\sigma_y^2 = \sum_{j=0}^{L-1}(j-\mu_y)^2\sum_{i=0}^{L-1} P_{ij}$
6	cluster shade	$f_6 = \sum_{i=0}^{L-1}\sum_{j=0}^{L-1}[(i-\mu_x)+(j-\mu_y)]^3 P_{ij}$
7	cluster prominence	$f_7 = \sum_{i=0}^{L-1}\sum_{j=0}^{L-1}[(i-\mu_x)+(j-\mu_y)]^4 P_{ij}$

Contrast is the difference between the highest and the lowest values of a contiguous set of pixels which indicate the variance of gray levels of the image. The GLCM contrast tends to be highly correlated with spatial frequencies while the module of the displacement vector tends to one. The low contrast image certainly features low spatial frequencies.

Entropy measures the disorder of an image. When the image is not texturally uniform, many GLCM elements have very small values, which imply that entropy is very large.

Energy is also called Angular Second Moment. Energy measures textural uniformity, i.e. pixel pairs repetitions. High energy value occurs when the gray level distribution over the window has either a constant or a periodic form.

Homogeneity is also called inverse difference moment. This parameter measures image homogeneity as it assumes larger values for smaller gray value differences in pair elements. Homogeneity decreases if contrast increases while energy is kept constant. On the other hand, it decreases if energy increases while contrast is kept constant.

Correlation is a measure of gray tone linear-dependencies in the image; in particular, the direction under investigation is the same as vector displacement. High correlation values imply a linear relationship between the gray levels of pixel pairs.

B. Gray level-gradient co-occurrence matrix

The GLCM method is commonly used example of this type of 2-D histogram. But the gray level-gradient co-occurrence matrix (GLGCM) takes into account the information of both gray level and gradient among each pixel in an image. The element $h(i, j)$ of GLGCM is defined ad the probability of the pixel number which has gray value i in the normalized gray image $F(m,n)$ and gradient value j in the normalized gradient image $G(m,n)$. Therefore, the gray level-gradient co-occurrence matrix provides the space relationship between each pixel and its adjacent pixel.

In the gas-liquid two phase flow image, Sobel operator with window-size of 3*3 was adopted to get the gradient image. Hence, the gradient normalized is shown as:

$$G(m,n) = INT[\, g(m,n)\times N_S / g_{max}\,] + 1 \quad (2)$$

Where, $g(m,n)$ is the gradient image, g_{max} is the maximum gradient value in matrix g. N_S is normalized maximum gradient value, for the presented study, we set $N_S = 16$.

Similarly, the gray levels normalize transformation is following formula (3):

$$F(m,n) = INT[\, f(m,n)\times N_g / f_{max}\,] + 1 \quad (3)$$

Where, $f(m,n)$ is the gray value image, f_{max} is the maximum gray value of matrix f. And N_g is the maximum gray value after normalization, set $N_g = 16$.

Then, count the number of pixels which satisfy $F(m,n) = i$ and $G(m,n) = j$, take it as H_{ij}. The total amount of H_{ij} were calculated by (4):

$$H = \sum_{i=1}^{Ng}\sum_{j=1}^{Ns} H_{ij} \quad (4)$$

Then the normalized GLGCM $\hat{H}_{ij}$ can be calculated by formula (5):

$$\hat{H}_{ij} = H_{ij} / (N_g \times N_s) \quad (5)$$

where, $i = 1,2,\cdots N_g$, $j = 1,2,\cdots N_s$.

Fifteen texture features can be proposed by Haralick et al [15]. Such as small-grads advantage, big-grads advantage, gray asymmetry, and so on. The feature computing formula is described in table 2. The

representative meaning for each parameter was not too much to explain here.

Table 2. Textural features by GLGCM

Serial No.	Texture Features	Calculating formula
1	Small Grads Dominance	$T_1 = \left[\sum_{i=1}^{Ng}\sum_{j=1}^{Ns}\frac{H_{ij}}{j^2}\right] / H$
2	Big Grads Dominance	$T_2 = \left[\sum_{i=1}^{Ng}\sum_{j=1}^{Ns} j^2 H_{ij}\right] / H$
3	Gray Asymmetry	$T_3 = \sum_{i=1}^{Ng}\left[\sum_{j=1}^{Ns} H_{ij}\right]^2 / H$
4	Grads Asymmetry	$T_4 = \sum_{j=1}^{Ns}\left[\sum_{i=1}^{Ng} H_{ij}\right]^2 / H$
5	Energy	$T_5 = \sum_{i=1}^{Ng}\sum_{j=1}^{Ns}\hat{H}_{ij}^2$
6	Gray Mean	$T_6 = \sum_{i=1}^{Ng} i\left[\sum_{j=1}^{Ns}\hat{H}_{ij}\right]$
7	Grads Mean	$T_7 = \sum_{j=1}^{Ns} j\left[\sum_{i=1}^{LNg}\hat{H}_{ij}\right]$
8	Gray Variance	$T_8 = \{\sum_{i=1}^{Ng}(i-T_6)^2\left[\sum_{j=0}^{Ns}\hat{H}_{ij}\right]\}^{\frac{1}{2}}$
9	Grads Variance	$T_9 = \{\sum_{j=1}^{Ns}(i-T_7)^2\left[\sum_{i=1}^{Ng}\hat{H}_{ij}\right]\}^{\frac{1}{2}}$
10	Correlation	$T_{10} = \sum_{i=1}^{Ng}\sum_{j=1}^{Ns}(i-T_6)(j-T_7)\hat{H}_{ij}$
11	Gray Entropy	$T_{11} = -\sum_{i=1}^{Ng}\left[\sum_{j=1}^{Ns}\hat{H}_{ij}\right] log_2\left[\sum_{j=1}^{Ns}\hat{H}_{ij}\right]$
12	Grads Entropy	$T_{12} = -\sum_{j=1}^{Ns}\left[\sum_{i=1}^{Ng}\hat{H}_{ij}\right] log_2\left[\sum_{i=1}^{Ng}\hat{H}_{ij}\right]$
13	Entropy	$T_{13} = -\sum_{i=1}^{Ng}\sum_{j=1}^{Ns}\hat{H}_{ij} log_2\hat{H}_{ij}$
14	Inertia	$T_{14} = \sum_{i=1}^{Ng}\sum_{j=1}^{Ns}(i-j)^2\hat{H}_{ij}$
15	Homogeneity	$T_{15} = \sum_{i=1}^{Ng}\sum_{j=1}^{Ns}\frac{1}{1+(i-j)^2}\hat{H}_{ij}$

III. EXPREMENT AND RESULTS

A. Experiment facility

The gas-water two-phase flow experiments were conducted at the Multi-phase Flow Laboratory of Tianjin University in China, as Fig. 1 illustrated.

The horizontal pipe is manufactured of Plexiglas, so that the flow regime and flow process could be observed more clearly in the experiment. The pipe is about 20m long and the inner diameter is 50mm. The total length of this pipeline between entrance nozzle and the outlet is approximately 16.56m, consists of two horizontal legs with the length of 7.22 and 7.30m respectively, connected by a horizontal U-bend with the length of 2.04m.

The volume flow rate of water is about 0.1-16.0 m^3/h, and gas is 0.06-82.0 m^3/h. The average temperature was 15.7 C°. Different flow regime could be formed by controlling the valve of water and gas pipe, such as bubble flow, plug flow, slug flow, wavy flow, annular flow and so on.

The multi-sensor system is installed at the downstream of the pipe where the flow regime is well developed and flow state is more stable.

A MiniVis ECO-2 high-speed video camera with frame rates up to 32000 fps was used to record the ascent bubbles in two phase flow. The biggest resolution of the camera is 1280×1024. However, higher spatial resolutions result in longer recording times and fewer video frames per unit time. A compromise between recording speed and image resolution has to be found. Experimentally, special resolution of 640×480 and frame frequency of 500 fps could satisfy the measurements and was adopted in all experiments reported in this study. Auxiliary backlighting with 5400K color temperature was also used as back light in the experiment. The camera is about 0.72m far from the front wall of pipeline. The effective shooting coverage is 50mm in vertical and 95mm in horizontal. The whole experiment system of gas-liquid two phase flow was shown as Fig. 1.

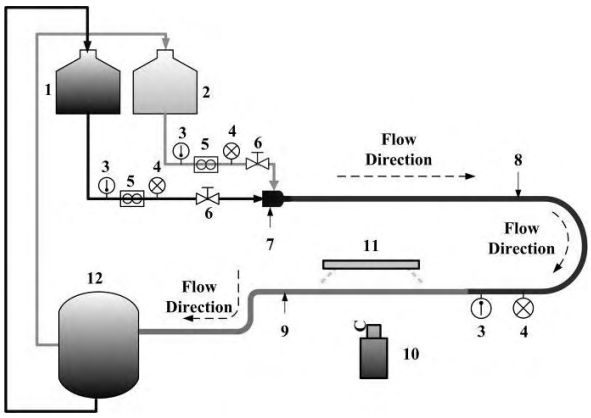

1 water tank; 2 gas tank; 3 Temperature; 4 Pressure Gauge; 5 Flow meter;
6 valve; 7 mixing ejector; 8 stainless Horizontal Pipe; 9 Perspex Horizontal Pipe; 10 high-speed camera; 11 light; 12 Separation Tank.

Fig. 1. Schematic view for the experimental system

B. Experimental results

(1) Gas/liquid flow images

Examples of gas/liquid two-phase flow experiment images, which at different superficial gas velocity (sg) and gas/liquid density ratio (dr), but with the same superficial liquid velocity (sl) about 1.26 m/s, were shown in Fig. 2:

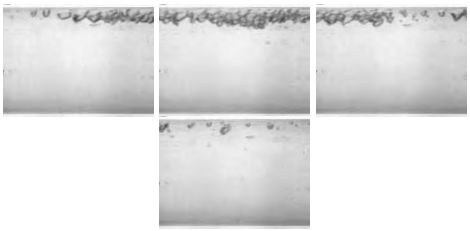

(a) case 1: sl=1.263m/s, sg =0.025m/s, dr=0.0018989

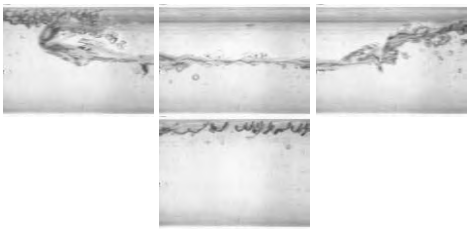

(b) case 2: sl=1.257m/s, sg =0.085m/s, dr=0.0019297

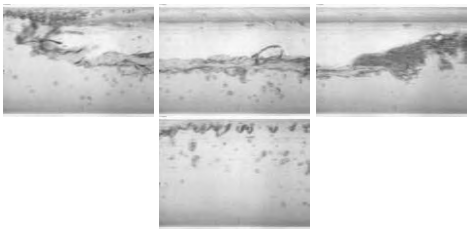

(c) case 3: sl=1.275m/s, sg =0.4192m/s, dr=0.0019182

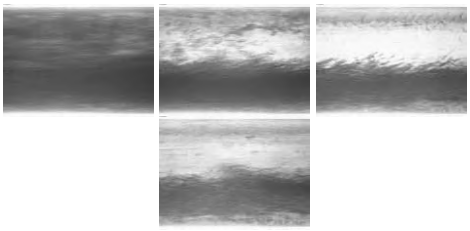

(d) case 4: sl=1.261m/s, sg =4.3171m/s, dr=0.0023790

Fig. 2. Gas/liquid two-phase flow images: sl: superficial liquid velocity; sg: superficial gas velocity; dr=gas/liquid density ratio.

30 images of each case were transformed into gray value image. They were denoised by both shadow subtraction method and wavelet filter. Then texture features of the 4 kinds flow images, which extract by GLCM and GLGCM separately, were compared in the following section.

(2) Texture features contrast

Textural features were extracted to measure useful information form gas-liquid flow images. All features which introduced in Table 1 and Table 2 were calculated in the research. Through contrasting, only the features which could reflect flow characters were shown in Fig 3 and Fig.4. For different flow case, they floated in a different rang which could distinguish each other.

All the textural features shown in Fig.3 and Fig.4 were orderliness to describe gas-liquid flow state. They were corresponding to the four case of Fig.2. To be observed, for the same superficial liquid velocity, almost every feature is close related to the gas/liquid density ratio but not the superficial gas velocity. Especially, for the same flow regime with the same superficial liquid velocity, the superficial gas velocity has nothing to do with the textural features, which was shown in case 2 and case 3.

In Fig. 3,Energy and homogeneity of GLCM are increasing with the gas/liquid density ratio. Entropy and cluster prominence of GLCM in Fig.3 are inversely proportional to gas/liquid density ratio. All of the four textural features did not reflect the changes of superficial gas velocity. Energy and entropy of the gas-liquid two phase flow images are well reflecting flow state than the other two for there are fewer junctions of the 4 flow cases.

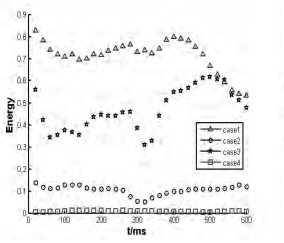

(a) energy

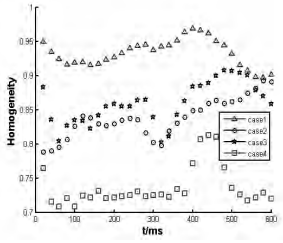

(b) homogeneity

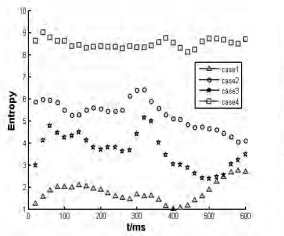

(c) entropy

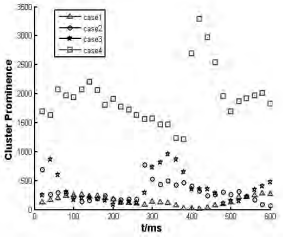

(d) cluster prominence

Fig. 3. Texture features of gas/liquid flow images got by GLCM

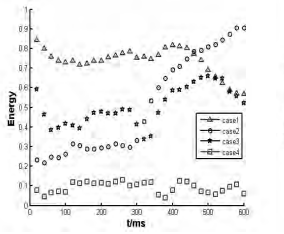

(a) energy

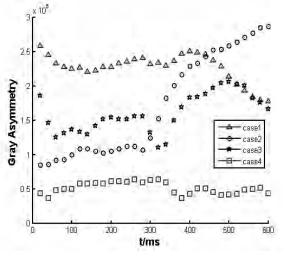

(b) gray asymmetry

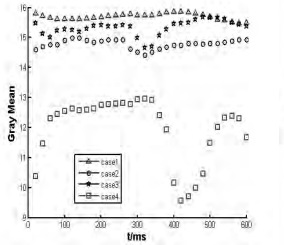

(c) gray mean

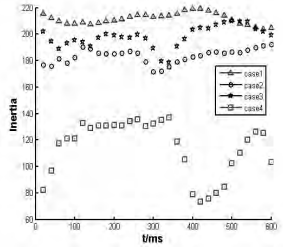

(d) Inertia

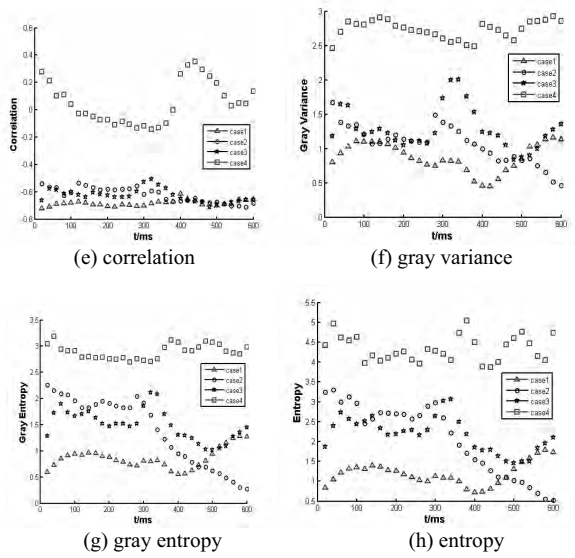

(e) correlation (f) gray variance

(g) gray entropy (h) entropy

Fig. 4. Texture features of gas/liquid flow images got by GLGCM

While in Fig. 4, energy, gray mean, inertia and correlation, which are calculated based on GLGCM, are increasing with the gas/liquid density ratio. Correlation, gray variance, gray entropy and entropy decrease when gas/liquid density ratio increasing. Practically, gray mean， Inertia and correlation have shown more regular than others. Either of the textural features has shown the relation to superficial gas velocity. For gas/liquid flow examples expect case 4 shown in this paper, the anaphase of the flow, with lesser gas, were the same as bubbly flow. Meanwhile, the features: gray mean ， Inertia and correlation were tending to meet at the same value. Therefore, the features of GLGCM not only can reflect the gas/liquid density ratio, but also can reflect the contents of gas in the flow to some extent. It can used to gas volumetric fraction measurement.

IV. CONCLUSION

Textural features method was used to analysis gas/liquid two-phase flow images which were captured by high speed camera. Both GLCM and GLGCM were detailed and texture features were introduced in the paper. Gas/liquid two-phase flow experiments were carried out at Multi-phase Flow Laboratory of Tianjin University. Experimental example, which was with 4 cases at the same superficial liquid velocity but different superficial gas velocity and gas/liquid density ratio, was presented to illuminate the relationship between the flow states and textural features. All features were extracted by GLCM and GLGCM. But, only the features which were regularly were shown in the paper. The results have shown that both GLCM and GLGCM were close related to the gas/liquid two-phase density. Therefore, these features could be used in flow regime recognition. Furthermore, gray mean ， Inertia and correlation, which based on GLGCM, well reflect the content of gas. They would be feasible in gas volume fraction measurement.

ACKNOWLEDGMENT

The author appreciates the support from National Natural Science Foundation of China (No. 50776063) and Program for New Century Excellent Talents in University of China (No. NCET-06-230).

REFERENCES

[1] G. F. Hewitt, Measurement of Two Phase Flow Parameters[M]. London and New York, Academic Press, 1978.

[2] M. Yang, H. I. Schlaberg, B. S. Hoyle, et al. "Parallel Image Reconstruction in Real-Time Ultrasound Process Tomography for Two-Phased Flow Measurements[J]". Real-time imaging, Vol. 3, No. 4, pp.295-303, Aug. 1997.

[3] J. J. Cilliers, W. Xie, S. J. Neething, et al. "Electrical Resistance Tomography Using a Bi-Directional Current Pulse Technique[J]", Meas. Sci. Techn., Vol. 12, No. 8, pp. 997-1001, Aug. 2001.

[4] S. Dutta, B. J. Barber, S. Parameswaran, "Texture Analysis of Protein Distribution Images to Find Differences[J]". Ann. Biomed. Eng., Vol. 23, No. 6, pp. 772-786, Nov. 1995.

[5] H. Q. Zhu, "The Segmentation Method of Retinal Blood Vessels Based on Gray Level-Gradient Co-occurrence Matrix[J]". J. Shanghai Jiao Tong U., Vol. 38, No.9, pp. 1485-1488, Sep. 2004.

[6] F. Z. Zhu and B. Wu, "B-Scan Ultrasonic Image Feature Extraction of Fatty Liver Based on Gray Level Co-occurrence Matrix[J]". Chin J. Med. Imaging Tech., Vol. 22, No.2, pp. 287-289, 2006.

[7] H. Q. Zhu, "Segmentation of Blood Vessels in Retinal Images Using 2-D Entropies of Gray Level-Gradient Co-occurrence Matrix[C]". Proceedings - IEEE International Conference on Acoustics, Speech and Signal Processing – Proceedings (ICASSP), Vol. 3, pp. III509-III512, 2004

[8] C. E. Honeycutt and R. S. Plotnick, "Image Analysis Techniques and Gray-Level Co-occurrence Matrices (GLCM) for Calculating Bioturbation Indices and Characterizing Biogenic Sedimentary Structures[J]". Comput. & Geosci., Vol. 34, No. 11, pp. 1461-1472, Nov. 2008.

[9] F. Kanda, M. Kubo and K. Muramoto, "Watershed Segmentation and Classification of Tree Species Using High Resolution Forest Imagery[J]". International Geoscience and Remote Sensing Symposium (IGARSS), Vol. 6, pp. 3822-3825, 2004

[10] J. Létal, D. Jirákb, L. uderlováa and M. Hájekb, "MRI 'Texture' Analysis of MR Images of Apples During Ripening and Storage[J]". Lebensmittel-Wissenschaft und-Technologie, Vol. 36, No. 7, pp. 719-727, Nov. 2003

[11] D. S. Xia, S. Jin and J. Wang, "Fractal Dimension and GGCM Meteorology Cloud Pictures Recognition". J. Nanjing U. Sci. Techn., Vol. 23, No. 4, pp. 289-292, Aug. 1999.

[12] L. Zhang and W. Lu, "Application of Segmentation Algorithm Based on Wavelet Mul-Scale Symbiotic Matrix in Residential Area Extraction[J]". J. Anhui Institute of Mechanical & Electrical Engineering, Vol. 17, No. 2, pp. 43-47, Jun. 2002.

[13] Y. L. Zhou, F. Chen and B. Sun, "Identification Method of Gas-Liquid Two-Phase Flow Regime Based on Gray Level Co-occurrence Matrix and Support Vector Machine[J]". J. Chem. Ind. Eng. (China), Vol. 58, No. 9, pp. 2232-2237, Sep. 2007.

[14] Z. Y. Wang, N. D. Jin, C. Wang and J. X. Wang, "Temporal and Spatial Evolution Characteristics of Two-phase Flow Pattern Based on Image Texture Analysis[J]". J. Chem. Ind. Eng. (China), Vol. 59, No. 5, pp. 1122-1130, May. 2008

[15] Haralick, K. Shanmugam and Its'hak Dinstein, "Textural Features for image classification[J]". IEEE T. . Syst. Man Cy. C., Vol. SMC-3, No. 6, pp. 610-621, Nov. 1973.